THE JOURNAL OF PHYSICAL CHEMISTRY C
A JOURNAL OF THE AMERICAN CHEMICAL SOCIETY

pubs.acs.org/JPCC
Article

Cation-Induced Dipole Moments on Single-Crystal Metal Surfaces

Published as part of The Journal of Physical Chemistry C special issue "Jacek Lipkowski Festschrift".

Fabiola Domínguez-Flores,* Axel Groß, and Wolfgang Schmickler

Cite This: J. Phys. Chem. C 2025, 129, 9179−9188
Read Online
ACCESS | Metrics & More | Article Recommendations

ABSTRACT: The properties of the electric double layer are largely determined by ions adsorbed on the electrode surface. To elucidate the role of cations in particular, we have studied hydrated Ca^{2+} and K^+ ions adsorbed on Pt(111), Au(111), and Ag(111) using density functional theory. In all the investigated cases, the cations are not chemisorbed on the metal electrode. A hybrid solvent model, combining implicit solvent with explicit water, was employed to accurately capture solvation effects. In this model, explicit water molecules form stable solvation cages around the ions, stabilizing their charge. These charges are balanced by the countercharge induced on the metal. The resulting dipole moment produces a dipole potential, which is determined by the solvation shell, the chemical interaction with the metal, and the screening properties of the metal. Notably, Ag(111) shows distinctive behavior, as its large electronic spillover results in smaller dipole moments. The dipole potential is seldom measured but can be related to the familiar electrosorption valency. While K^+ practically retains its charge upon adsorption, Ca^{2+} shows a true partial charge transfer, resulting in a fractional electrosorption valency.

1. INTRODUCTION

Since the advent of surface science, it has been recognized that adsorbates on metal surfaces may acquire a partial charge, which is balanced by a counter-charge on the metal surface.[1] This arrangement of charges results in a dipole moment, which modifies the work function of the metal.[2,3] Prime examples are adsorbed alkali and halide ions, which are well investigated.[4−9] Early density functional calculations showed that the counter charge, otherwise known as the image charge, spills over the geometrical metal surface and may even partially surround the adsorbate.[10] This implies that the dipole moment is influenced not only by the charge transfer to the adsorbate but also by the screening properties of the metal.

The same principle applies in electrochemical adsorption processes,[11] where the initial state is usually an ion from the solution, whereas in surface science it is an atom in the gas phase. Despite this difference, the behavior of the adsorbed state remains similar. A significant difference in electrosorption, however, is the presence of the solvent, which is usually polar, as in the case of water. The dipole moments of the solvent molecules interact with the charge on the adsorbate and may modify or screen it, making electrosorption more complicated. Additionally, electrosorption is affected by the electrode potential, generating a measurable current, which led to the concept of electrosorption valency.[12]

Adsorbed water molecules also influence the surface charge distribution of bare metal surfaces, predominantly through electronic redistribution, with a small contribution from the orientational dipole of the water molecules.[13] The orientation of the water molecules at the interface is specific to each metallic surface, with well-known configurations at the potential of zero charge (PZC).[14,15] These configurations influence thermodynamic properties at the interface, driven by both energetic and entropic factors.[16]

Electrochemical experiments related to the dipole moment generated by the adsorbate are challenging, and data remain scarce. However, not only are the charges on the adsorbates and their screening by the metal and the solvent key factors in understanding electrochemical adsorption, but they also strongly influence on the local reaction conditions for electrocatalytic reactions. For instance, halide ions affect hydrogen evolution, and in alkaline solutions, the same reaction as well as CO_2 reduction can be catalyzed by cations which are not chemically adsorbed.[17,18] In particular, the presence of cations can significantly influence the dipole generated at the electrode surface, mainly through charge transfer interactions and solvent reorganization.[19−21]

Due to their great importance in electrochemistry, there have been countless studies of ions or atoms in the electrical double layer on an electrode surface. In recent years, most of this work has been based on DFT.[22−25] A significant challenge reported in these studies is the modeling of the solvent. Ideally, solvents should be treated at the same atomic level as the

Received: February 16, 2025
Revised: April 11, 2025
Accepted: April 23, 2025
Published: May 5, 2025

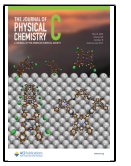

https://doi.org/10.1021/acs.jpcc.5c01062
J. Phys. Chem. C 2025, 129, 9179−9188

Table 1. Pt, Au, and Ag with 1/9 Ca Coverage, and Effect of the Implicit Solvent[a]

surface	work function pristine surface [V]	$\Delta\phi$ [V]	dipole moment [e Å]	Bader charge	adsorption distance [Å]
(3 × 3)Pt(111)	5.52	2.65	0.91	1.3	2.2
(3 × 3)Pt(111) + imp solv	5.31	3.14	1.07	1.3	2.6
(3 × 3)Au(111)	4.91	2.25	0.85	1.3	2.1
(3 × 3)Au(111) + imp solv	4.70	2.29	0.87	1.7	2.2
(3 × 3)Ag(111)	4.17	1.67	0.64	1.1	2.4
(3 × 3)Ag(111) + imp solv	3.90	2.84	1.09	1.8	2.8

[a]$\Delta\phi$: work function difference between the system of reference without the ion and the system with the ion. Work functions are for the adsorption of a single atom. Dipole = $\Delta\phi\epsilon_0 A$.

Table 2. Pt, Au, and Ag Interaction with 1/9 K Coverage, and Effect of Implicit Solvent[a]

surface	work function pristine surface [V]	$\Delta\phi$ [V]	dipole moment [e Å]	Bader charge	adsorption distance [Å]
(3 × 3)Pt(111)	5.52	3.07	1.05	0.80	2.8
(3 × 3)Pt(111) + imp solv	5.31	2.00	0.68	0.96	3.6
(3 × 3)Au(111)	4.91	2.75	1.04	0.70	2.8
(3 × 3)Au(111) + imp solv	4.70	1.94	0.74	0.99	4.7
(3 × 3)Ag(111)	4.17	2.36	0.90	0.70	2.9
(3 × 3)Ag(111) + imp solv	3.90	1.75	0.67	0.99	4.8

[a]$\Delta\phi$: (see Table 1).

electrode and statistically averaged over different solvent configurations. However, this is computationally too expensive. A hybrid approach, combining an implicit solvent model with explicit water molecules, offers a feasible solution. While implicit solvation models effectively capture macroscopic properties such as electrostatic screening, long-range solvent effects, and bulk solvent characteristics[26−28], the inclusion of explicit water molecules is crucial for an accurate ion representation at the interface.[29,30] Moreover, explicit water molecules are essential to account for partial charge transfer due to solvation shell polarization, highlighting the limitations of implicit models in such situations.[31,32] Nonetheless, fully explicit solvent models are computationally prohibitive for complex reaction mechanisms. Thus, a hybrid approach, where a limited number of explicit solvent molecules are integrated into a continuum model, allows for a treatment of solvent and ion effects at the interface.[33] In this work, we aim to enhance our understanding of adsorption on metal electrodes by studying two ions with different charges, Ca^{2+} and K^+, on commonly used electrode materials, such as Pt(111), Au(111), and Ag(111), using a hybrid approach. Like many metal cations, these ions are not chemically adsorbed on these metals, so that the interactions are dominated by charge transfer, dipole formation, and electrostatic effects. These cations are small and have a low polarizability so that, unlike in the case of anion adsorption, the polarizability plays a negligible role.

2. METHODS

We conducted periodic DFT calculations using the Vienna ab initio simulation package (VASP).[34,35] As previously demonstrated,[36] the revised Perdew−Burke−Ernzerhof (RPBE) exchange−correlation functional,[37] combined with the DFT-D3 dispersion correction method developed by Grimme et al.,[38] provides reliable accuracy to model the electrochemical interface between a metal electrode and an aqueous electrolyte, particularly with the inclusion of dispersion corrections based on the zero-damping scheme. The electronic cores were represented using the projector-augmented wave (PAW) method,[39] and the electronic states were expanded using a plane wave basis set with a cutoff energy of 400 eV.

Three single crystal electrodes were modeled as a six-layer (3 × 3)-FCC(111) slab, with the two innermost layers fixed at an optimized lattice parameter of 3.99, 4.21, 4.19 Å, for Pt(111), Au(111) and Ag(111), respectively. The two outermost layers on each side of the slab were fully relaxed until the forces on each atom were less than 10^{-6} eV/Å. Gamma-centered *k*-point meshes were generated with a reciprocal space resolution of (3 × 3 × 1). The adsorbed atoms, K and Ca, were placed over each surface in their preferred adsorption sites, which for both atoms are hcp hollow sites (with minimum difference to fcc), leading to a perfectly symmetric system, with 1/9 coverage. To simulate long-range interactions with the solvent, we used the implicit solvent model as implemented in the VASPsol package,[40,41] with a permittivity value of 78.4 and a surface tension parameter $\tau = 0$, since we aimed to compare the three metals on a purely electrostatic basis. Two configurations of the solvation shell were tested for each atom: one with six molecules surrounding the atom and another with seven. A 20 Å thick implicit solvation layer was applied along the surface-normal axis of the slab to prevent interactions between the slab and its periodic images in the upper and lower directions.

Favorable orientations of water molecules were explored to generate an appropriate solvation shell around each ion by means of DFT-MD simulated annealing, using a linear temperature ramp heating the system from 0 to 370 K in 2 ps, followed by another ramp to cool it from 370 to 0 K in 2.5 ps, using a Nosé−Hoover thermostat; this method was applied to both ions over all surfaces. The final orientations of the water-molecule configurations were used to optimize the solvation shell with 6 and 7 water molecules.

The balance of the countercharge due to the electron transfer caused by the ion-surface interaction generates a measurable dipole moment,[42] which we can obtain by analyzing changes produced in the work function from the surfaces with an adsorbate. While initially it may seem straightforward to calculate the dipole moment using the expression: $\mu = Qd$, where Q is the charge and d is the ion-surface distance, this method overlooks several important

https://doi.org/10.1021/acs.jpcc.5c01062
J. Phys. Chem. C 2025, 129, 9179−9188

Table 3. Pt, Au, and Ag Interaction with 1/9 Ca Coverage under Different Conditions: Six Water Molecules and Implicit Solvent[a]

surface	work function surface [V]	$\Delta\phi$ [V]	dipole moment [e Å]	Bader charge	adsorption distance [Å]
(3 × 3)Pt(111) + water	5.57	3.36	1.15	1.6	2.9
(3 × 3)Pt(111) + water + imp solv	5.41	2.51	0.86	1.6	2.9
(3 × 3)Au(111)+ water	5.14	2.87	1.09	1.6	2.8
(3 × 3)Au(111) + water + imp solv	4.79	2.47	0.94	1.6	3.0
(3 × 3)Ag(111) + water	4.81	2.73	1.05	1.6	2.8
(3 × 3)Ag(111) + water + imp solv	4.25	2.38	0.91	1.6	3.0

[a]$\Delta\phi$: (see Table 1).

Table 4. Pt, Au, and Ag Interaction with 1/9 Ca Coverage under Different Conditions: Seven Water Molecules and Implicit Solvent[a]

surface	Work Function surface [V]	$\Delta\phi$ [V]	dipole moment [e Å]	Bader charge	distance [Å]
(3 × 3)Pt(111) + water	5.69	2.07	0.71	1.6	2.9
(3 × 3)Pt(111) + water + imp solv	4.67	2.57	0.88	1.7	4.1
(3 × 3)Au(111)+ water	4.83	2.17	0.82	1.6	3.0
(3 × 3)Au(111) + water + imp solv	4.77	3.13	1.19	1.7	4.3
(3 × 3)Ag(111) + water	4.22	2.12	0.81	1.6	3.0
(3 × 3)Ag(111) + water + imp solv	4.22	2.71	0.96	1.7	4.2

[a]$\Delta\phi$: (see Table 1).

Table 5. Pt, Au, and Ag Interaction with 1/9 K Coverage under Different Conditions: Implicit Solvent, Six Water Molecules, and the Combined Environment[a]

surface	work function surface [V]	$\Delta\phi$ [V]	dipole moment [e Å]	Bader charge	adsorption distance [Å]
(3 × 3)Pt(111) + water	5.99	1.54	0.53	0.88	3.6
(3 × 3)Pt(111) + water + imp solv	5.29	1.86	0.64	0.96	6.0
(3 × 3)Au(111) + water	5.07	1.52	0.58	0.89	3.6
(3 × 3)Au(111) + water + imp solv	4.72	1.72	0.65	0.96	6.0
(3 × 3)Ag(111) + water	4.80	2.04	0.78	0.88	3.6
(3 × 3)Ag(111) + water + imp solv	4.12	1.93	0.74	0.96	6.0

[a]$\Delta\phi$: (see Table 1).

Table 6. Pt, Au, and Ag Interaction with 1/9 K Coverage under Different Conditions: Implicit Solvent, Seven Water Molecules, and the Combined Environment[a]

surface	work function surface [V]	$\Delta\phi$ [V]	dipole moment [e Å]	Bader charge	adsorption distance [Å]
(3 × 3)Pt(111) + water	5.92	1.87	0.64	0.90	3.6
(3 × 3)Pt(111) + water + imp solv	5.19	1.65	0.56	0.94	5.0
(3 × 3)Au(111) + water	5.36	1.90	0.72	0.90	3.8
(3 × 3)Au(111) + water + imp solv	4.72	1.69	0.64	0.95	5.0
(3 × 3)Ag(111) + water	4.47	1.46	0.56	0.90	4.0
(3 × 3)Ag(111) + water + imp solv	3.95	1.52	0.52	0.95	5.0

[a]$\Delta\phi$: (see Table 1).

factors. To accurately calculate the dipole moment, one must account for the surface area (A), the effect of the solvent, and the potential difference $\Delta\phi$ relative to a reference system. Given these considerations, the dipole moment is more precisely expressed as $\Delta\phi\epsilon_0 A$. Where $\Delta\phi$ is the work function difference between the system of reference without the ion and the system with the ion, and A is the surface area. In the presence of an implicit solvent, there is no vacuum in our system, so the work function was calculated from the potential at large distances from the metal within the implicit solvent. The implicit solvent is a pure dielectric, and hence does not have a surface potential; so the potential is the same on both sides of the surface of an implicit solvent.

We report the changes in the work function for three different metallic crystalline surfaces and two ions placed on the surface at their preferred positions (from Tables 1, 2, 3, 4, 5, and 6). The top side of Figure 1 shows one electron potentials and the work functions for a pristine (3 × 3)Pt(111) surface resulting from interactions under various conditions, including the presence of an implicit solvent, water molecules, and their combined effect. The bottom side of the figure shows the interactions involving the ion alone, ion with implicit solvent, ion with water, and ion with both the implicit solvent and water are depicted in the right part of the figure. These potentials are averaged parallel to the electrode surface. Therefore, the potential generated by the water molecules only generates minor wiggles, since the hydrogen and oxygen potentials tend to cancel each other. In contrast, the attractive potential generated by adsorbed Ca^{2+} is clearly visible on the bottom part of the figure, second plot.

https://doi.org/10.1021/acs.jpcc.5c01062
J. Phys. Chem. C 2025, 129, 9179−9188

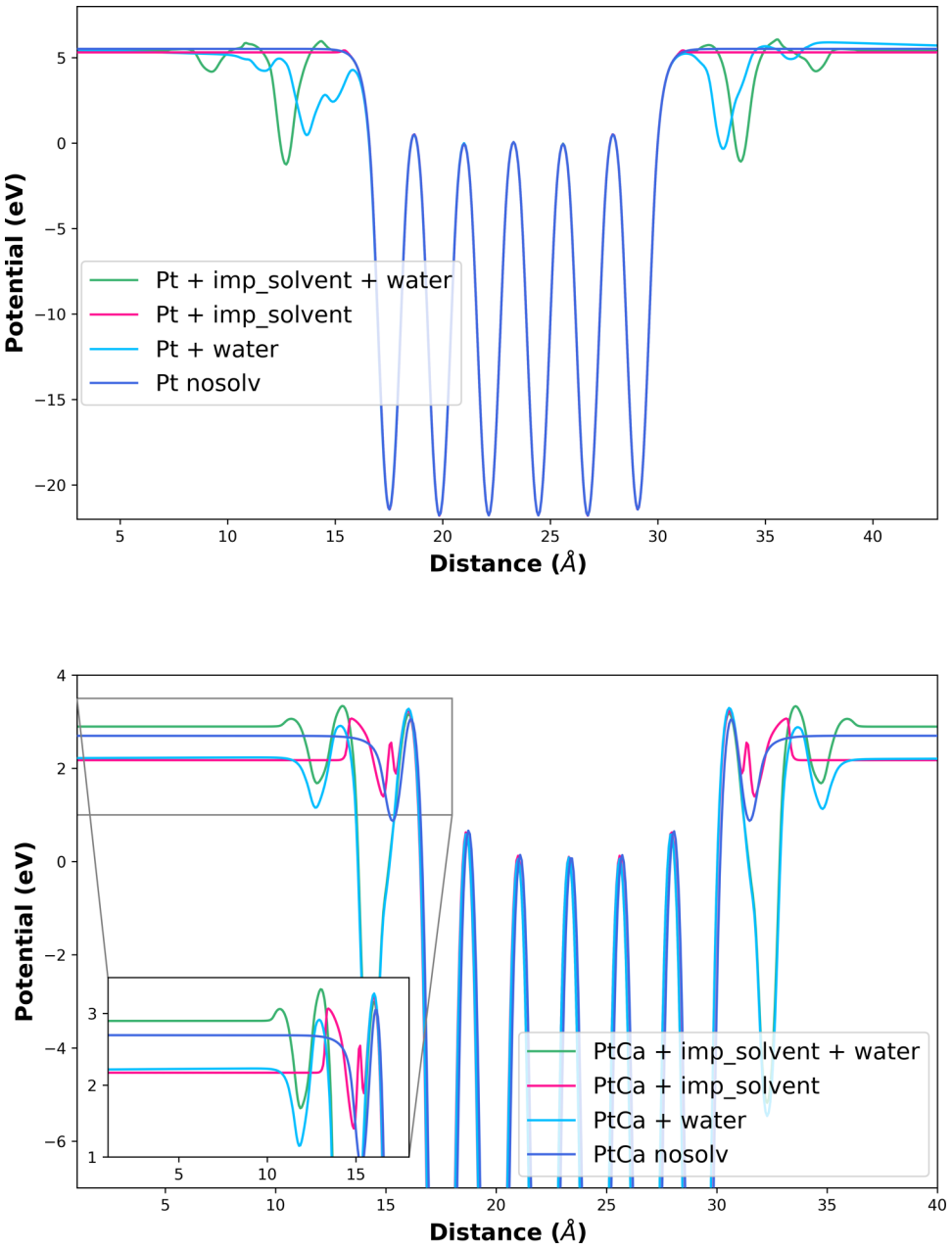

Figure 1. Top: (3 × 3)Pt(111), bottom: Ca/(3 × 3)Pt(111). At various conditions: with an implicit solvent, with water, and both combined.

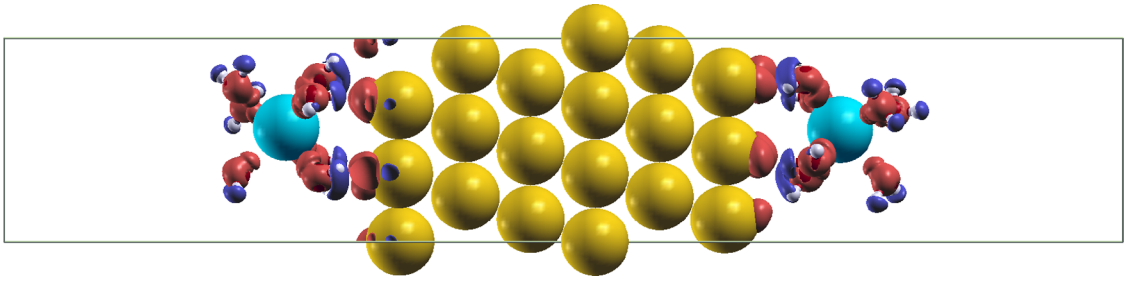

Figure 2. Charge density difference of the side view of Ca/(3 × 3)Au(111) + 7 water molecules. The blue region depicts positive charge, and the red negative charge. Isovalue of ±0.001 e Å^3.

As illustrated in the inset panel of Figure 1, second plot, one might expect that combining implicit and explicit solvents would lower the electrostatic potential, as both individually reduce the electrostatic potential compared with the cation alone on the surface. However, the total interfacial dipole and the vacuum reference shift can behave in a nonintuitive manner. In the specific case of Pt, this combination of solvent models appears to increase the dipole at the interface. On

https://doi.org/10.1021/acs.jpcc.5c01062
J. Phys. Chem. C 2025, 129, 9179−9188

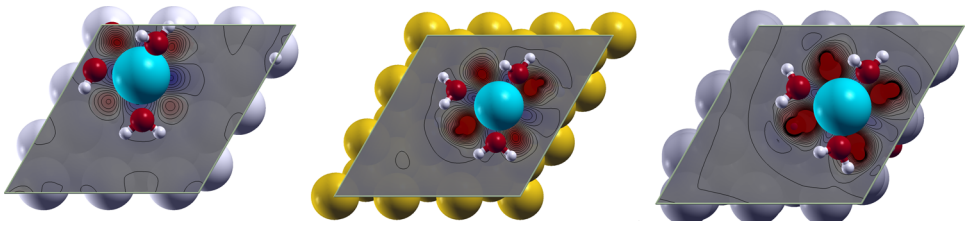

Figure 3. Charge density difference (Ca/(3 × 3)Ag(111), Ca/(3 × 3)Au(111), Ca/(3 × 3)Pt(111)) + 7 water molecules, top plane-cut with three water molecules above the plane and four below. Blue region depicts positive charge and red negative charge. Isovalue of ± 0.001 e Å^3.

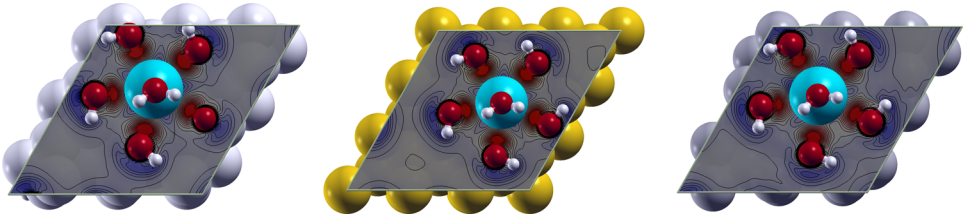

Figure 4. Charge density difference (Ca/(3 × 3)Ag(111), Ca/(3 × 3)Au(111), Ca/(3 × 3)Pt(111)) + 6 water molecules, top plane-cut. Isovalue of ±0.001 e Å^3.

surfaces like Pt(111), the electronic response to adsorbates is particularly sensitive thus, small changes in the arrangement of water molecules can lead to noticeable shifts in the local potential, making the overall effect less predictable than the effects on Au or Ag, which do not noticeably change the electrostatic potential.

To calculate the dipole moment for each system, we compared the potential differences between the reference system and the ion-containing systems for each case. The dipole moment observed is affected across all of the metallic surfaces, depending on the reaction conditions and the ion-specific surface interactions. As seen in Figure 2, the implicit solvent and the polarization of water molecules exert opposing influences on the effective position of the image plane. An analysis of the counter charge density reveals that the charge is predominantly localized on the surface, with a residual negative charge remaining near the water molecules; see Figures 2 and 3, calculated as $\rho_{diff} = \rho_{ion+water+surface} - \rho_{ion} - \rho_{water} - \rho_{surface}$. Consequently, the charge calculated using the Bader method deviates from an integer value (Tables 1 and 2), which is an expected outcome due to the complexity of charge distribution in these systems.

3. RESULTS AND DISCUSSION

3.1. Solvation Shell. Our main objective was to construct an ideal solvation shell that accurately captures short-range interactions at the interface while remaining compatible with an implicit solvent model to account for long-range interactions. Previous studies have shown that the first solvation shell of cations typically contains six to eight water molecules.[32,43,44] To refine the structure and orientation of the water molecules within this solvation shell, we performed DFT-MD simulations. After optimizing configurations with varying numbers of water molecules around both Ca^{2+} and K^+, we determined that the optimal solvation shell for these ions consists of either six or seven water molecules. The solvation shells were fully optimized at 0 K in both cases. Hence, our calculations are static, which could be perceived as a considerable constraint. However, the solvation shells of alkali and earth alkali ions are quite stable. The residence times of water molecules in the first hydration shells of alkali ions are of the order of tens of picoseconds,[45] and for the divalent ions, they are even longer, so that our calculations should capture the essence of the adsorbate properties.

3.1.1. Structure of the Six-Water Solvation Shell. In the configuration with six water molecules, the solvation shell exhibited a nearly symmetric arrangement. Five water molecules are equidistant from the ion and from themselves, and have one hydrogen pointing toward the surface and the other toward the next water molecule. The sixth water molecule was placed horizontally on top of the ion. This star-like arrangement is particularly interesting as it suggests the apparent adsorption of a semisolvated Ca^{2+} on the surface, see Figure 4. While it is generally accepted that cations do not specifically adsorb on the surface until very negative potentials are applied,[25] other studies suggest that the presence of water on the surface can enhance the adsorption of smaller cations while weakening that of larger ones.[46] We observed a similar behaviour in the presence of six water molecules, Ca^{2+} was contact adsorbed on all the FCC(111) surfaces we tested, whereas K^+ was not contact adsorbed in the hybrid solvation model; see discussion below.

3.2. Role of the Considered Cations in the Adsorption Process. For our two prime models, six or seven water molecules plus implicit solvent, the adsorption geometries are very similar for the three metals. The size of the cation plays a significant role in its interaction with the surface. Larger cations like K^+ tend to disrupt hydrogen bonding within the solvation shell, leading to a delocalized and less stable positive charge compared to smaller cations such as Ca^{2+}. Charge transfer is determined by several factors: ionization energies of the atom, solvation energy, image charge, and the work function of the substrate. K has a low first energy of ionization, 4.34 eV, which is lower than the work function of the metals considered. Therefore, it is easily ionized and carries a high positive charge, which is close to unity when it is solvated. A higher positive charge is prohibited by the high second energy of ionization of 31.7 eV. The first ionization energy of Ca, 6.22 eV, is somewhat larger than the work function of the metals considered. But image interaction and solvation induce a positive charge. Indeed, because of its relatively low second energy of ionization, 11.8 eV, it acquires fractional charges

https://doi.org/10.1021/acs.jpcc.5c01062
J. Phys. Chem. C 2025, 129, 9179−9188

Figure 5. Charge density difference for Ca/(3 × 3)Ag(111): with implicit solvent (right) and vacuum (left). Isovalue of ± 0.0005 e Å^3.

larger than unity. Because of their low density of valence electrons, they interact primarily through electrostatic forces and image charge effects. Because K^+ and Ca^{2+} are hard, weakly polarizable cations, their adsorption distances remain relatively short compared to those when they are surrounded by one more molecule.

When the K^+ shell is formed by seven water molecules plus implicit solvent, its distance to the surface decreases to 5 Å, compared to 6 Å with six water molecules, indicating a stronger interaction. In contrast, the opposite trend is observed for Ca^{2+}, where the distance increases to 4 Å with seven water molecules and decreases to 3 Å with six water molecules. This reduction in adsorption distance is likely due to enhanced charge stabilization within the solvation shell and the concomitant stronger attraction to the surface (comparisons done considering only results obtained from the hybrid configuration; see Tables 3−6).

3.3. Dipole Moments in the Vacuum. Before analyzing the effects of solvation, it is useful to establish a reference system by first considering adsorption in vacuum. Tables 1 and 2 summarize the relevant quantities for Ca and K adsorption on Pt(111), Au(111), and Ag(111), including dipole moments, adsorption distances, and Bader charges. The latter should be interpreted cautiously, as the metal electrons that screen the adsorbate charge partially surround the ion,[10] complicating an accurate charge evaluation.

Essentially, three critical factors affect the dipole moments in the following systems: (1) The work function of the metal: a higher work function means a stronger attraction of the electrons and hence a larger positive charge on the adsorbate. (2) The screening properties of the metal: the ability of the metal to screen the charge can be characterized by the position of the effective image plane.[10] The further this plane is in front of the metal surface, the better the adsorbate charge is screened. For the three metals under consideration, the distances between adsorbate and metal are larger for Ag, which exhibits the best screening ability among these metals.[47] A better screening reduces the total dipole moment. (3) Adsorption distance: a larger distance between the adsorbate and the metal surface results in a larger dipole moment, since dipole moments are proportional to both charge and separation distance.

3.3.1. Adsorption of Calcium. It is important to realize that the dipole moments are caused not only by the adsorbed particle but also by the whole interface. The Bader charges and dipole moments on Pt and Ag are roughly equal. Based on the higher work function of Pt, one would expect a higher charge on the ion adsorbed on this surface, but as discussed above, Bader charges may not fully capture the effective charge. Also, the Pauling electron affinity of Au (2.54) is higher than that of Pt (2.28). The adsorption distance on Pt(111) is somewhat larger than in Au(111), so is the dipole moment; similarly, the adsorption distance on Ag(111) + implicit solvent is larger and consequently is the dipole moment. The most important finding in this table is the small dipole moment on Ag in vacuum, which is caused by both the good screening property of this metal and the small work function.

3.3.2. Adsorption of Potassium. The dipole moments for potassium follow the same trend: the values for Pt(111) and Au(111) are roughly equivalent, while Ag(111) displays a smaller dipole moment. Interestingly, the Bader charges for K on Au(111) and Ag(111) are nearly the same, which might seem unexpected. However, as with calcium, these values should be treated with caution due to the limitations of the Bader charge approximation in this context.

3.4. Solvation Effects. *3.4.1. Implicit Solvent.* Basically, an implicit solvent adds a background dielectric constant to the part of the system that is not occupied by atoms. Similar to the famous dark matter in cosmology, it cannot be imaged directly but can be detected by its effects on the system. On bare metal surfaces, the implicit solvent leads to a small reduction of the work function, of the order of 0.2−0.3 eV. The implicit solvent screens the spillover of the electrons into the vacuum, thereby reducing the work function. This effect has already been observed in the jellium model,[48] where it is somewhat larger, since the spillover extends further.

The implicit solvent forms a solvation shell around the adsorbed ions. To a first approximation, the solvation energy is proportional to the square of the charge. So the solvent induces a strong tendency to increase the charge on the adsorbate in all cases. In the case of K, the adsorbate is almost completely ionized. At the same time, it reduces the dipole moment and weakens the electrostatic interaction with the metal substrate, so that the adsorption distance becomes larger. This effect is particularly large for K, which carries a unit charge and is therefore more weakly bound than Ca. Indeed, in this case, the adsorption distance changes up to almost 2 Å. But even for Ca on Ag(111) this shift is of the order of 0.4 Å and is related to the increase in the positive charge by 0.7. Figure 5 shows the charge distribution for Ca adsorbed on Ag(111) in the absence (left) and presence (right) of an implicit solvent. In the latter case, the charge on the adsorbate is significantly larger, and it is further from the surface; this

https://doi.org/10.1021/acs.jpcc.5c01062
J. Phys. Chem. C 2025, 129, 9179−9188

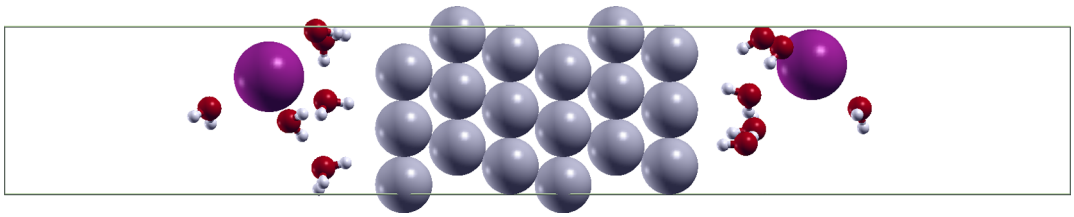

Figure 6. Side view of K/Pt(111) + 6 water molecules.

induces a spreading out of the pancake-like countercharge on the silver surface.

Since the implicit solvent itself has no energy, it is easy to calculate the hydration energy of the adsorbed ions. It varies a little between the various metals, but since the implicit solvent is a rough approximation in any case, we are only interested in average values. For adsorbed K^+, the solvation energy is about 2.6 eV, to be compared with the experimental value for K^+ in the bulk of 3.6 eV.[49] Therefore, about 1/3 of the hydration energy gets lost on adsorption, which seems reasonable for geometric reasons. However, this contradicts the findings of Quaino et al.,[50] who studied adsorption by classical molecular dynamics. They observed no change in the hydration energy upon adsorption since the water forms a very favorable hydration shell. Obviously, such structural effects are missing in an implicit solvent. On the other hand, classical molecular dynamics is based on effective interactions, which lack quantum molecular details.

For adsorbed calcium, our calculations predict a hydration energy of about 5 eV, much smaller than the bulk value of 16.6 eV.[49] The implicit solvent model, which is based on a linear response, is too simple for multivalent ions. Note that a theoretical study addressing the adsorption of iodide near a water/metal interface, using a combination of quantum chemical cluster calculations, the Newns−Anderson theory of chemisorption, and molecular dynamics simulations,[51] found two different ionic adsorption states separated by a small energy barrier. We did, in fact, not observe two separate adsorption states. We associate this difference to the fact that, in general, the interaction of anions with metal surfaces is stronger than that of cations.

3.4.2. Explicit and Hybride Solvation. We calculated the dipole moments of Ca^{2+} and K^+ ions over the Pt, Au, and Ag metallic surfaces in the presence of an explicit solvent, which, as previously discussed, could consist of either six or seven water molecules. In a second step, we combined explicit and implicit solvents.

In this section, we focus on how different environmental conditions affect the dipole moments. In principle, modeling a solvation shell differs from a single water layer, as the arrangement of the water molecules and their respective dipoles contributes distinctly to the overall dipole moment, either from the water dipole moment or, as in our case, the dipole moment from the adsorbate.

Water molecules arrange differently depending mainly on the ion rather than on the surface. This is illustrated in Figure 6, where the alignment of water molecules around K^+ is less symmetrical compared to the highly ordered arrangement observed with Ca^{2+}. Because of its smaller charge, the hydration shell of K^+ is less rigid.

For clarity, we separated the dipole moment calculations by ion type and by the number of water molecules in the solvation shell. The corresponding values for both Ca and K under the six-water-molecule condition are presented in Tables 3−6. Just as the implicit solvent, the water tends to reduce the overall dipole moment by a net orientation of the hydrogen toward the surface. On the other hand, solvation tends to increase the charge and pull the ion toward the bulk, which has the opposite effect on the dipole moment. This makes it difficult to understand the overall effect.

3.4.3. Ca^{2+} Dipole Moments. This ion is compact and carries a double charge, which leads to a close-packed, symmetric arrangement of water molecules when the solvation shell is formed by six molecules. In this configuration, one water molecule is positioned horizontally over the surface (on top of the ion), while the remaining five surround the ion, each with one hydrogen atom pointing toward the surface. The dipole moment trend observed only with water is Pt > Au > Ag. However, when an implicit solvent model is applied, the trend changes to Au > Ag > Pt. The distance between the Pt surface and the ion is smaller than with the other two metals, resulting in a smaller dipole moment.

When the ion is surrounded by seven water molecules, the arrangement becomes less compact, with the water molecules distributed above and below the ion. In the case of Pt, the water molecules below the ion typically have one hydrogen pointing toward the surface. For Ag, however, some water molecules have different geometries above the surface. The dipoles generated by the water molecules pointing directly at the surface contribute to the overall dipole moment, which is influenced by each metal's screening properties. As a result, the dipole moments for Pt and Ag are smaller compared to those for Au in this configuration. In general, the trend shows an increasing dipole moment for all metals. However, Pt appears to be particularly sensitive to local environmental changes compared to Au or Ag. With six water molecules, the interfacial water structure is more ordered (as shown in Figure 4), maximizing the surface dipole moment. The addition of a seventh water molecule disrupts this arrangement, resulting in a less oriented water network and a weaker overall dipole. On Pt, where adsorbate interactions are highly dependent on coordination and electronic structure, even subtle changes can significantly reduce the efficiency of charge transfer stabilization.

In the four cases investigated, the Bader charge is larger than in the vacuum and takes on a value of 1.6−1.7. In addition, the adsorption distance is greater.

3.4.4. K^+ Dipole Moments. Since the unit charge of this ion does not promote the formation of a compact shell, the water molecules are positioned farther from the ion. Despite this, the hydrogen atoms of the molecules beneath the ion are mostly oriented to the surface, with their angles showing no significant deviation compared to their arrangement around the Ca^{2+}. Therefore, the effect of the water dipole is, on average, similar to the effect faced by Ca^{2+}. Interestingly, the dipole moment values for this ion display an opposite trend: Ag > Au > Pt

https://doi.org/10.1021/acs.jpcc.5c01062
J. Phys. Chem. C 2025, 129, 9179−9188

when considering only the water molecules. When the implicit solvent is introduced, the trend remains consistent with what was observed in the six-water-molecule case, with Ag maintaining the highest dipole moment. When the ion is surrounded by seven water molecules, the trend in dipole moment values shifts to Au > Pt > Ag, which remains unchanged even with the addition of the implicit solvent. This outcome is expected given that silver consistently exhibits the lowest dipole moment in such configurations. The more surprising result arises from the six-water-molecule case, where silver presents the highest dipole moment, diverging from the expected behavior. The potential difference is always lower with an arrangement of six water molecules, because at the interface, this arrangement creates an ordered network, aligning the water dipoles that effectively counteract the surface electric field from the metal, which results in a decrease in the electrostatic potential. When an extra water molecule is added, it disturbs this ordered network, leading to a less oriented overall dipole. Consequently, the screening becomes less effective, and the potential drop increases.

3.5. Dipole Moment and Electrosorption Valency.

Measuring the dipole moment μ of an adsorbate experimentally is challenging, and available data are limited, making direct comparisons difficult. Moreover, when changes in the dipole moment occur due to an applied potential, it is necessary to introduce a related concept: the electrosorption valency γ, defined as the charge that flows onto the electrode surface per adsorbed particle at constant electrode potential ϕ:

$$e_0\gamma = \left(\frac{\partial\sigma}{\partial\Gamma}\right)_{\phi} \tag{1}$$

where σ is the surface charge density on the electrode, and Γ is the surface excess of the adsorbate. Obviously, the electrosorption valency can only be determined in a complete electrochemical system with a solution and a double layer. As discussed above, within DFT, this is impossible to model by a discrete solvent, and the major part of the solution must be modeled implicitly. A good explanation of how this can be done is detailed elsewhere.[52]

An equation proposed by Vetter and Schultze[53] relates the electrosorption valence to the nonmeasurable charge $\lambda = z - q$ transferred during adsorption, where z is the charge number of the ion:

$$\gamma = gz - \lambda(1 - g) \text{ where } g = \left(\frac{\partial\phi_{ad}}{\partial\phi}\right)_{\Gamma} \tag{2}$$

g is called a geometrical factor, which gives the change in the potential ϕ_{ad} at the adsorbate site with the electrode potential. According to Schultze and Koppitz,[54] $g = 0.16 - 0.84\lambda/z$. Since λ is negative, we have $0 \le g \le 1$.

Let us start the discussion with K^+. Eq 2 allows us to estimate the electrosorption valency from the charge transfer. In the presence of any water model, the charge on adsorbed K^+ is almost unity on all three metals. If we use an average value of about 0.95, we obtain $\gamma \approx 0.24$. The only experimental value for K^+ is on Hg with $\gamma = 0.16$,[54] which is based on the assumption that $\lambda = 0$; overall, this is a satisfactory agreement.

For the electrosorption of Ca^{2+}, the charge on the adsorbate does not vary much between the three metals. If we use an average value of $\lambda = -0.31$, we obtain an estimate of $\gamma \approx 0.8$, indicative of a physical partial charge transfer. Unfortunately, there are no experimental values, but our estimate may be useful in future experiments.

At the potential of zero charge (pzc), the dipole moment and the electrosorption valency are related through:

$$\mu = \frac{ze_0\epsilon_0}{C_H}(1 - \gamma/z) \tag{3}$$

where C_H is the Helmholtz capacity of the double-layer, and ϵ_0 the permittivity of vacuum. This equation, which is based on a linear response, shows explicitly that the experimental dipole moment depends on the double-layer capacity, which characterizes the screening properties of the interface. In particular, a large capacity indicates good screening of charges and results in small dipole moments. Conversely, a small electrosorption valency implies a small charge transfer, a large remaining charge on the ion, and hence a large dipole moment. In eq 2, the double-layer properties are contained in the geometric factor. Eq 3 is not based on any model for the double layer but purely on thermodynamic reasoning. There are two different and equivalent derivations in refs 3 and 55.

For a given Helmholtz capacity, eq 1, which is based on the linear response, suggests a maximum value for the dipole moment: $\mu_{max} = ze_0\epsilon_0/C_H$. For example, for $z = 1$ and $C_H = 0$, 1 F m^{-2}, this gives a value of $0.88e_0$ Å, which is in fact larger than all the dipole moments calculated for K^+. For Ca^{2+}, with $z = 2$, the limiting value would be twice as large and thus again higher than all the values we obtained for this ion. As has been discussed by Avila et al.,[56] obtaining the Helmholtz capacity requires a full model of the system, including the electrolyte; nevertheless, an inspired estimate can be useful to check the consistency of the results. In fact, $C_H = 0.1$ F m^{-2} is a decent estimate for this purpose since cations are usually adsorbed at low negative potentials, where the Helmholtz capacities are of this order of magnitude. Using for K^+ an average value of $\mu \approx 0.65e_0$ Å for all three metals, we obtain an estimate of $\gamma \approx 0.28$, which compares quite well with the value of 0.24 obtained above from an entirely different argument. For Ca^{2+}, the dipole moments scatter somewhat for the different metals, but a value of $\mu \approx 0.9e_0$ Å is a good average, which results in $\gamma \approx 1$. This is only slightly higher than the value estimated from eq 2. More importantly, both methods predict correctly that the electrosorption valency of K^+ is low in all cases, indicating little charge transfer, while that of Ca^{2+} is substantially higher, indicating true partial charge transfer.

Schultze and Koppitz[54] also propose a relation for the electrosorption valency based on differences in the electron affinities. However, with the chosen parameters, this works quite well for the absorption of anions. All the halides investigated by these authors are chemisorbed on the surface, so the properties of the chemical bond are captured by electronegativities, which describe the chemical bonding. In contrast, the cations studied in this work are not chemically bonded; therefore, we refrain from a discussion in terms of electron affinities.

4. CONCLUSIONS

We have investigated the adsorption of two different atoms (Ca and K), that, after interacting with the surface, can be considered as the divalent Ca^{2+} and the monovalent K^+, on the popular electrode surfaces Pt(111), Au(111) and Ag(111), by means of DFT. In all cases investigated, there was no chemical bonding of the adsorbates, as we have discussed at length in

https://doi.org/10.1021/acs.jpcc.5c01062
J. Phys. Chem. C 2025, 129, 9179−9188

the introduction; solvation of adsorbed cations presents a special problem. To address this, we have employed various models: simple implicit solvation, ensembles of explicit water with 6 and 7 molecules, and a combination of these ensembles with implicit solvent. Our results show a complex interplay between solvation and attraction from the metal: Solvation favors a high charge on the adsorbate, and a larger adsorption distance, so that the solvent can surround the adsorbate as far as possible. While these effects tend to increase the dipole moment, the orientation of the explicit water and the implicit solvent tends to shield the overall dipole moment. The metal attracts the adsorbate through a combination of chemical interaction and image forces. The image charge spills over from the metal surface and compensates for the charge on the ion. These opposing effects, solvation-driven repulsion and metal-driven attraction, prevent the establishment of a clear universal trend, necessitating a case-by-case analysis for each metal surface.

This spillover effect is particularly large on silver, so that the surface dipole moments induced by the adsorbates tend to be smaller on this metal. This is in line with the fact that the surface-enhanced Raman effect is strong on silver, where, indeed, it has been discovered,[57] indicating a strong response of the surface electrons to external fields. This is consistent with DFT calculations,[47] which showed a substantially stronger response for Ag than for Au or Pt.

Adsorbate dipole moments are rarely measured in electrochemistry; they are, however, related to the electrosorption valency. Unfortunately, this relation involves an electric double layer, which is absent in our model. Nevertheless, by using reasonable values for the capacity, we estimated consistent values for the electrosorption valencies from two different relations. The small value of $\gamma \approx 0.24-0.26$ for K^+ indicates ionic adsorption with little charge transfer, while the larger values of $\gamma \approx 0.88-1$ for Ca^{2+} indicate true partial charge transfer.

AUTHOR INFORMATION

Corresponding Author

Fabiola Domínguez-Flores − *Institute of Theoretical Chemistry, Ulm University, 89081 Ulm, Germany;* orcid.org/0000-0002-0102-6240; Email: fabiola-1.dominguez-flores@uni-ulm.de

Authors

Axel Groß − *Institute of Theoretical Chemistry, Ulm University, 89081 Ulm, Germany;* orcid.org/0000-0003-4037-7331

Wolfgang Schmickler − *Institute of Theoretical Chemistry, Ulm University, 89081 Ulm, Germany;* orcid.org/0000-0003-4162-6010

Complete contact information is available at: https://pubs.acs.org/10.1021/acs.jpcc.5c01062

Notes

The authors declare no competing financial interest.

ACKNOWLEDGMENTS

We acknowledge support by the state of Baden-Württemberg through bwHPC, and the German Research Foundation (DFG) through grant no INST 40/575-1 FUGG (JUSTUS 2 cluster). W.S. gratefully acknowledges support by the ESTATIK Stiftung Günter&Sylvia Lüttgers.

REFERENCES

(1) Kolasinski, K. W. *Surface science*, 4th edition; John Wiley & Sons: Nashville, TN, 2020.

(2) Gross, A. *Theoretical Surface Science*, 2nd edition; Springer: Berlin, Germany, 2009.

(3) Bange, K.; Straehler, B.; Sass, J. K.; Parsons, R. The interaction of br with ag (110): comparison of electrochemical and gas-phase adsorption measurements. *Journal of Electroanalytical Chemistry and Interfacial Electrochemistry* **1987**, *229* (1), 87−98.

(4) Gossenberger, F.; Roman, T.; Groß, A. Equilibrium coverage of halides on metal electrodes. *Surf. Sci.* **2015**, *631*, 17−22. Surface Science and Electrochemistry - 20 years later.

(5) Gossenberger, F.; Roman, T.; Groß, A. Hydrogen and halide co-adsorption on pt(111) in an electrochemical environment: a computational perspective. *Electrochim. Acta* **2016**, *216*, 152−159.

(6) Frumkin, A. N. Influence of cation adsorption on the kinetics of electrode processes. *Trans. Faraday Soc.* **1959**, *55*, 156−167.

(7) Pan, B.; Wang, Y.; Li, Y. Understanding and leveraging the effect of cations in the electrical double layer for electrochemical co2 reduction. *Chem. Catalysis* **2022**, *2* (6), 1267−1276.

(8) Shah, A. H.; Zhang, Z.; Huang, Z.; Wang, S.; Zhong, G.; Wan, C.; Alexandrova, A. N.; Huang, Y.; Duan, X. The role of alkali metal cations and platinum-surface hydroxyl in the alkaline hydrogen evolution reaction. *Nat. Catal.* **2022**, *5* (10), 923−933.

(9) Resasco, J.; Chen, L. D.; Clark, E.; Tsai, C.; Hahn, C.; Jaramillo, T. F.; Chan, K.; Bell, A. T. Promoter effects of alkali metal cations on the electrochemical reduction of carbon dioxide. *J. Am. Chem. Soc.* **2017**, *139* (32), 11277−11287. PMID: 28738673.

(10) Lang, N. D. Small adsorbate dipole moments need not imply small charge transfers. *Surf. Sci. Lett.* **1983**, *127* (2), L118−L122.

(11) Schmickler, W.; Guidelli, R. The partial charge transfer. *Electrochim. Acta* **2014**, *127*, 489−505.

(12) Vetter, K. J.; Schultze, J. W. Stromfluß bei elektrosorption-sprozessen und elektrosorptionswertigkeit. *Berichte der Bunsengesellschaft für physikalische Chemie* **1972**, *76* (9), 927−933.

(13) Li, X.-Y.; Chen, A.; Yang, X.-H.; Zhu, J.-X.; Le, J.-B.; Cheng, J. Linear correlation between water adsorption energies and volta potential differences for metal/water interfaces. *J. Phys. Chem. Lett.* **2021**, *12* (30), 7299−7304. PMID: 34319117.

(14) Le, J.; Cuesta, A.; Cheng, J. The structure of metal-water interface at the potential of zero charge from density functional theory-based molecular dynamics. *J. Electroanal. Chem.* **2018**, *819*, 87−94.

(15) Toney, M. F.; Howard, J. N.; Richer, J.; Borges, G. L.; Gordon, J. G.; Melroy, O. R.; Wiesler, D. G.; Yee, D.; Sorensen, L. B. Voltage-dependent ordering of water molecules at an electrode−electrolyte interface. *Nature* **1994**, *368* (6470), 444−446.

(16) Domínguez-Flores, F.; Kiljunen, T.; Groß, A.; Sakong, S.; Melander, M. M. Metal-water interface formation: Thermodynamics from abinitio molecular dynamics simulations. *J. Chem. Phys.* **2024**, *161* (4), No. 044705.

(17) Gebremariam, G. K.; Jovanovic, A. Z.; Pašti, I. A. The effect of electrolytes on the kinetics of the hydrogen evolution reaction. *Hydrogen* **2023**, *4* (4), 776−806.

(18) Ringe, S. Cation effects on electrocatalytic reduction processes at the example of the hydrogen evolution reaction. *Current Opinion in Electrochemistry* **2023**, *39*, No. 101268.

(19) Santos, E.; Schmickler, W. The potential of zero charge of a metal electrode and the surface potential of water from simulations. *Current Opinion in Electrochemistry* **2023**, *38*, No. 101208.

(20) Schwarz, K.; Groenenboom, M. C.; Moffat, T. P.; Sundararaman, R.; Vinson, J. Resolving the geometry/charge puzzle of the c(2 × 2)-cl cu(100) electrode. *J. Phys. Chem. Lett.* **2021**, *12* (1), 440−446. PMID: 33356303.

(21) Waegele, M. M.; Gunathunge, C. M.; Li, J.; Li, X. How cations affect the electric double layer and the rates and selectivity of electrocatalytic processes. *J. Chem. Phys.* **2019**, *151* (16), 160902.

(22) Li, P.; Huang, J.; Hu, Y.; Chen, S. Establishment of the potential of zero charge of metals in aqueous solutions: Different faces

of water revealed by ab initio molecular dynamics simulations. *J. Phys. Chem. C* **2021**, *125* (7), 3972−3979.
(23) Otani, M.; Sugino, O. First-principles calculations of charged surfaces and interfaces: A plane-wave nonrepeated slab approach. *Phys. Rev. B* **2006**, *73*, No. 115407.
(24) Le, J.-B.; Fan, Q.-Y.; Li, J.-Q.; Cheng, J. Molecular origin of negative component of helmholtz capacitance at electrified pt(111)/water interface. *Sci. Adv.* **2020**, *6* (41), No. eabb1219.
(25) Magnussen, O. M.; Groß, A. Toward an atomic-scale understanding of electrochemical interface structure and dynamics. *J. Am. Chem. Soc.* **2019**, *141* (12), 4777−4790.
(26) Cramer, C. J. *Essentials of computational chemistry*, 2nd edition; John Wiley & Sons: Chichester, UK, 2004.
(27) Tomasi, J.; Mennucci, B.; Cammi, R. Quantum mechanical continuum solvation models. *Chem. Rev.* **2005**, *105* (8), 2999−3094. PMID: 16092826.
(28) Fattebert, J.-L.; Gygi, F. First-principles molecular dynamics simulations in a continuum solvent. *Int. J. Quantum Chem.* **2003**, *93* (2), 139−147.
(29) Hörmann, N. G.; Guo, Z.; Ambrosio, F.; Andreussi, O.; Pasquarello, A.; Marzari, N. Absolute band alignment at semiconductor-water interfaces using explicit and implicit descriptions for liquid water. *npj Comput. Mater.* **2019**, *5* (1), 100.
(30) Bramley, G.; Nguyen, M.-T.; Glezakou, V.-A.; Rousseau, R.; Skylaris, C.-K. Reconciling work functions and adsorption enthalpies for implicit solvent models: A pt (111)/water interface case study. *J. Chem. Theory Comput.* **2020**, *16* (4), 2703−2715. PMID: 32182065.
(31) Horinek, D.; Herz, A.; Vrbka, L.; Sedlmeier, F.; Mamatkulov, S. I.; Netz, R. R. Specific ion adsorption at the air/water interface: The role of hydrophobic solvation. *Chem. Phys. Lett.* **2009**, *479* (4), 173−183.
(32) Santos, E. How cations catalyse the hydrogenation of graphene vacancies. *Electrochim. Acta* **2024**, *497*, No. 144532.
(33) Gauthier, J. A.; Ringe, S.; Dickens, C. F.; Garza, A. J.; Bell, A. T.; Head-Gordon, M.; Nørskov, J. K.; Chan, K. Challenges in modeling electrochemical reaction energetics with polarizable continuum models. *ACS Catal.* **2019**, *9* (2), 920−931.
(34) Kresse, G.; Furthmüller, J. Efficiency of ab-initio total energy calculations for metals and semiconductors using a plane-wave basis set. *Comput. Mater. Sci.* **1996**, *6* (1), 15−50.
(35) Kresse, G.; Furthmüller, J. Efficient iterative schemes for ab initio total-energy calculations using a plane-wave basis set. *Phys. Rev. B* **1996**, *54*, 11169−11186.
(36) Sakong, S.; Forster-Tonigold, K.; Groß, A. The structure of water at a Pt(111) electrode and the potential of zero charge studied from first principles. *J. Chem. Phys.* **2016**, *144* (19), 194701.
(37) Hammer, B.; Hansen, L. B.; Nørskov, J. K. Improved adsorption energetics within density-functional theory using revised Perdew-Burke-Ernzerhof functionals. *Phys. Rev. B* **1999**, *59*, 7413.
(38) Grimme, S.; Antony, J.; Ehrlich, S.; Krieg, H. A consistent and accurate ab initio parametrization of density functional dispersion correction (DFT-D) for the 94 elements H-Pu. *J. Chem. Phys.* **2010**, *132* (15), 154104.
(39) Blöchl, P. E. Projector augmented-wave method. *Phys. Rev. B* **1994**, *50*, 17953−17979.
(40) Mathew, K.; Sundararaman, R.; Letchworth-Weaver, K.; Arias, T. A.; Hennig, R. G. Implicit solvation model for density-functional study of nanocrystal surfaces and reaction pathways. *J. Chem. Phys.* **2014**, *140* (8), No. 084106.
(41) Mathew, K.; Kolluru, V. S. C.; Mula, S.; Steinmann, S. N.; Hennig, R. G. Implicit self-consistent electrolyte model in plane-wave density-functional theory. *J. Chem. Phys.* **2019**, *151* (23), 234101.
(42) Lang, N. D.; Kohn, W. Theory of metal surfaces: Work function. *Phys. Rev. B* **1971**, *3*, 1215−1223.
(43) Persson, I. Hydrated metal ions in aqueous solution: How regular are their structures? *Pure Appl. Chem.* **2010**, *82* (10), 1901−1917.
(44) Waluyo, I.; Huang, C.; Nordlund, D.; Bergmann, U.; Weiss, T. M.; Pettersson, L. G. M.; Nilsson, A. The structure of water in the hydration shell of cations from x-ray Raman and small angle x-ray scattering measurements. *J. Chem. Phys.* **2011**, *134* (6), No. 064513.
(45) Koneshan, S.; Rasaiah, J. C.; Lynden-Bell, R. M.; Lee, S. H. Solvent structure, dynamics, and ion mobility in aqueous solutions at 25 °c. *J. Phys. Chem. B* **1998**, *102* (21), 4193−4204.
(46) McCrum, I. T.; Hickner, M. A.; Janik, M. J. Quaternary ammonium cation specific adsorption on platinum electrodes: A combined experimental and density functional theory study. *J. Electrochem. Soc.* **2018**, *165* (2), F114.
(47) Luque, N. B.; Schmickler, W. The electric double layer on graphite. *Electrochim. Acta* **2012**, *71*, 82−85.
(48) Schmickler, W. The potential of zero charge of jellium. *Chem. Phys. Lett.* **1983**, *99* (2), 135−139.
(49) Bard, A. J; Parsons, R.; Jordan, J. *Standard Potentials in Aqueous Solution*; Routledge, 2017.
(50) Schmickler, W.; Belletti, G.; Quaino, P. The approach of alkali ions towards an electrode surface - a molecular dynamics study. *Chem. Phys. Lett.* **2022**, *795*, No. 139518.
(51) Nazmutdinov, R. R.; Spohr, E. Partial charge transfer of the iodide ion near a water/metal interface. *J. Phys. Chem.* **1994**, *98* (23), 5956−5961.
(52) Hörmann, N. G.; Marzari, N.; Reuter, K. Electrosorption at metal surfaces from first principles. *npj Comput. Mater.* **2020**, *6* (1), 136.
(53) Schultze, J. W.; Vetter, K. J. Experimental determination and interpretation of the electrosorption valency. *J. Electroanal. Chem. Interfacial Electrochem.* **1973**, *44* (1), 63−81.
(54) Koppitz, F. D.; Schultze, J. W. Bond formation in electrosorbates−ii electrosorption and double layer properties in non-aqueous solvents. *Electrochim. Acta* **1976**, *21* (5), 337−343.
(55) Schmickler, W.; Santos, E. *Interfacial Electrochemistry*, 2nd edition; Springer: Berlin, Germany, 2010.
(56) Ávila, M.; Juárez, M. F.; Santos, E. Role of the partial charge transfer on the chloride adlayers on au(100). *ChemElectroChem.* **2020**, *7* (20), 4269−4282.
(57) Fleischmann, M.; Hendra, P. J.; McQuillan, A. J. Raman spectra of pyridine adsorbed at a silver electrode. *Chem. Phys. Lett.* **1974**, *26* (2), 163−166.

https://doi.org/10.1021/acs.jpcc.5c01062
J. Phys. Chem. C 2025, 129, 9179−9188